Hybrid Digital Pre-distortion for Active Phased Arrays Subject to Varied Power and Steering Angle

Li, Yunfeng; Huang, Yonghui; Chen, Qingyue; Jalili, Feridoon; Olesen, Kasper Bruun ; Gjedsted Brask, Jakob; Føns Dyring, Lauge; Pedersen, Gert Frølund; Shen, Ming

Published in:
I E E E Microwave and Wireless Components Letters

DOI (link to publication from Publisher):
10.1109/LMWC.2022.3172215

Publication date:
2022

Document Version
Accepted author manuscript, peer reviewed version

Hybrid Digital Pre-Distortion for Active Phased Arrays Subject to Varied Power and Steering Angle

Yunfeng Li, *Student Member, IEEE*, Yonghui Huang, Qingyue Chen, Feridoon Jalili, Kasper B. Olesen, Jakob G. Brask, Lauge F. Dyring, Gert F. Pedersen, *Senior Member, IEEE*, and Ming Shen, *Senior Member, IEEE*

***Abstract*— This letter proposes a memory polynomial (MPM)-aided deep neural network (DNN) digital pre-distortion (MaD-DPD) method for active phased arrays (APAs) subject to varied input power and steering angle. This has been challenging for traditional array linearization methods using either MPM or DNN, which rely on the in-phase and quadrature-phase (I/Q) signal as input and output to derive model parameters. In comparison, the proposed method actively incorporates MPM and DNNs to achieve linearization. The model uses only two varied APA state parameters (input power and steering angle) as input and the MPM coefficients as regression target, eliminating the need for model parameter updating. The MaD-DPD method is validated using a four-by-four antenna array at 28 GHz with 21 input power levels and a broad range of steering angles from −78° to 78°, improving up to 13.16% in error vector magnitude (EVM) and 18.21 dBc in adjacent channel leakage ratio (ACLR).**

***Index Terms*— Active phased array (APA), deep neural network (DNN), memory polynomial (MPM), MPM-aided DNN digital pre-distortion (MaD-DPD).**

I. Introduction

THE increasing demand for spectrum efficiency has triggered advances in millimeter-wave (mm-Wave) technology. The high path loss and beamforming issues of mm-Wave make phased arrays the focus of attention [1]. The array implementations usually have a separate transmit power amplifier (PA) to drive each antenna element. The PA's efficiency and linearity are among the key drivers to reduce energy consumption while enabling high data rates in the satellite communication, fifth generation (5G), and beyond 5G mm-Wave phased array transmitters. To maximize the available output power of each PA with high efficiency, the PA must operate in a nonlinear region [2]. However, the nonlinearity of PA will cause adjacent channel power leakage and deteriorate the error vector magnitude (EVM) of the transmission signal [3], [4].

Manuscript received April 2, 2022; accepted April 25, 2022. This work was supported by the China Scholarship Council under Grant 202004910734. *(Corresponding author: Yonghui Huang.)*

Yunfeng Li and Qingyue Chen are with the National Space Science Center, Chinese Academy of Sciences, Beijing 100190, China, and also with the School of Electronic, Electrical and Communication Engineering, University of Chinese Academy of Sciences, Beijing 100049, China (e-mail: yli@es.aau.dk).

Yonghui Huang is with the National Space Science Center, Chinese Academy of Sciences, Beijing 100190, China (e-mail: yonghui@nssc.ac.cn).

Feridoon Jalili, Kasper B. Olesen, Jakob G. Brask, Lauge F. Dyring, Gert F. Pedersen, and Ming Shen are with the Department of Electronic Systems, Aalborg University, 9220 Aalborg, Denmark (e-mail: mish@es.aau.dk).

Color versions of one or more figures in this letter are available at https://doi.org/10.1109/LMWC.2022.3172215.

Digital Object Identifier 10.1109/LMWC.2022.3172215

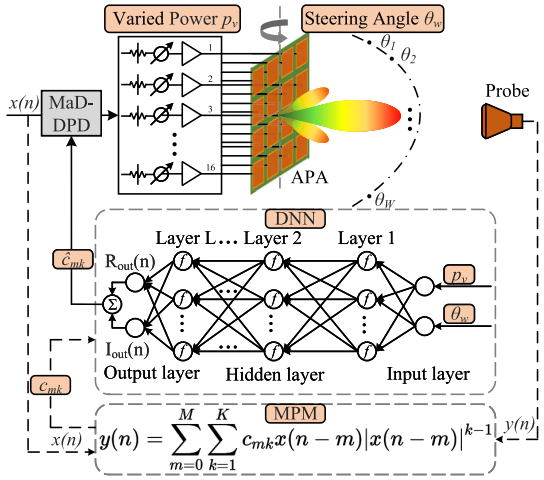

Fig. 1. Concept illustration of the MaD-DPD method for APA subject to varied input power and steering angle. Coefficients c_{mk} and $\hat{c}_{mk}$ are for DNN training and application, respectively.

Therefore, linearization is necessary to achieve the linearity and efficiency required by an active phased array (APA) operating under mm-Wave.

The representative linearization techniques with different polynomial-based digital pre-distortion (DPD) solutions have been proposed in [5]–[8]. As an alternative to polynomial-based DPD methods, deep neural networks (DNNs) can also offer effective linearization solutions due to their excellent nonlinear modeling capabilities [4], [9]–[11]. However, both the traditional array linearization methods and DNN-based DPD methods rely on the in-phase and quadrature-phase (I/Q) signal as input and output to derive model parameters. The nonlinear characteristics of the array will change with varied input power and steering angle. Therefore, the DPD systems given under certain conditions rely on I/Q signals, and they may not be suitable for real-time beam-direction updating. The beam direction can be updated at a millisecond level in 5G new radio (NR) [12]. Therefore, a high-efficiency update adaptation DPD can be challenging under large signal bandwidths in the frequency range of two (FR2: 24–52.6 GHz) systems.

This letter presents a memory polynomial (MPM)-aided DNN digital pre-distortion (MaD-DPD) method for APA, constructed using only two variable state parameters (input power and steering angle) as input and the MPM coefficient as regression target, as shown in Fig. 1. The proposed method is not a lookup table as the trained DNN can handle unlimited unseen power levels and steering angles. The DNN acts as a nonlinear function that directly generates the correct MPM coefficients for DPD instead of capturing and processing the I/Q data

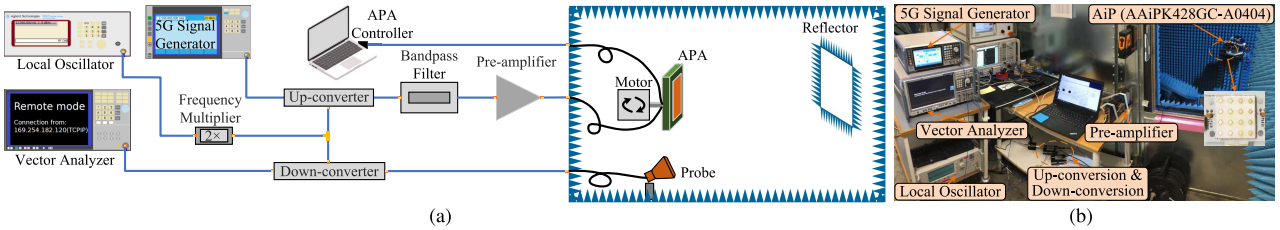

Fig. 2. Measurement setup. (a) Block diagram of measurement setup in the compact range chamber. (b) Photograph of the experiment setup.

in the real application. Although the APA exhibits distinct nonlinear characteristics for every input power and steering angle, the proposed MaD-DPD can significantly reduce the computational complexity and improve the updating efficiency.

II. Proposed MaD-DPD Method

The proposed MaD-DPD framework consists of one input, one output, and multiple hidden layers. In general, the generalization ability of DNN increases exponentially with the depth of layers [13]. The MPM is used to model the nonlinear APA

$$y(n) = \sum_{m=0}^{M} \sum_{k=1}^{K} c_{mk} x(n-m)|x(n-m)|^{k-1} \tag{1}$$

where M and K denote the memory depth and the MPM order, respectively. Variable c_{mk} represents the coefficient of MPM, and the detailed calculation process can be found in [14]. The normalized mean square error (NMSE) estimation method is used for the MPM coefficient calculation [15]. The combination of all coefficients can be expressed as

$$C_{MK} = [c_{01}, \ldots, c_{mk}, \ldots, c_{MK}]. \tag{2}$$

A. Operation of Each Layer

1) Input Layer (Two Neurous):

$$P_{\text{in}} = \begin{bmatrix} p_1 & p_2 & \cdots & p_v \end{bmatrix} \tag{3}$$

$$A_{\text{in}} = \begin{bmatrix} \theta_1 & \theta_2 & \cdots & \theta_w \end{bmatrix}. \tag{4}$$

The input layer with two neurons is composed of variable input power P_{in} and steering angle A_{in}.

2) Hidden Layer (l = 1, 2, ..., L, J^l Neurons):

$$h_i^{(l)} = f\left(\sum_{j=1}^{J} \alpha_{i,j}^{(l)} x_j^{(l-1)} + b_i^{(l)} \right) \tag{5}$$

where $h_i^{(l)}$ is the output of the ith neuron in the lth layer, and $\alpha_{i,j}^{(l)}$ is the weight connecting the jth neuron in the $(l-1)$th layer to the ith neuron in the lth layer. The bias term $b_i^{(l)}$ is used as an additional input for the ith neural in the lth layer. The hidden layers use the Sigmoid activation function [16].

3) Output Layer ($l = L + 1$, 2 Neurons):

$$R_{\text{out}} = h_1^{(L+1)} = \sum_{j=1}^{J} \alpha_{1,j}^{(L+1)} x_j^{(L)} + b_1^{(L+1)} \tag{6}$$

$$I_{\text{out}} = h_2^{(L+1)} = \sum_{j=1}^{J} \alpha_{2,j}^{(L+1)} x_j^{(L)} + b_2^{(L+1)} \tag{7}$$

$$C_{MK} = R_{\text{out}} + i\, I_{\text{out}}. \tag{8}$$

The outputs R_{out} and I_{out} are the real and imaginary components of the MPM's coefficient C_{MK}, respectively. It should be noted that DNNs cannot operate with complex numbers, and all MaD-DPD outputs are organized into a $2 \times MK$ vector.

Algorithm 1 MaD-DPD Training Procedure

Step 1: Capture the input and output signal from the compact range chamber under varied input power and steering angle;
Step 2: Generate the data set based on (1) and (2);
Step 3: Train the MaD-DPD with input (3) and (4), output (10) until the MSE loss reaches a preset value or convergence;
Step 4: Save the coefficients obtained from MaD-DPD for verification.

B. MaD-DPD Training Procedure

For the MaD-DPD training procedure, as shown in Algorithm 1, the input power varies from −30 to −20 dBm with a resolution of 0.5 dBm, resulting in $v = 21$. The steering azimuth angle is selected from −78° to 78° with $w = 17$ (0°, ±8°, ±15.5°, ±23.5°, ±32.5°, ±41.5°, ±52°, ±64.5°, ±78°). Therefore, there are $21 \times 17 = 357$ groups in total, where nearly 76% are used for training, 19% for testing, and 5% for validation. Each group obtains the MPM coefficient with a memory depth of 11 and an order of 3. Each group's MPM coefficients are $11 \times 3 = 33$ complex numbers. The parameters of learning rate, batch size, and epoch for the MaD-DPD are set to be 0.01, 100, and 1000, respectively. There are four hidden layers, each of which has 256 neurons. The mean squared error (MSE) loss function is used, as it is defined by

$$\text{loss} = \frac{1}{2B} \sum_{n=1}^{B} \left(\left(R_{\text{out}}(n) - \hat{R}_{\text{out}}(n) \right)^2 + \left(I_{\text{out}}(n) - \hat{I}_{\text{out}}(n) \right)^2 \right) \tag{9}$$

where B is the batch size of MaD-DPD. $\hat{R}_{\text{out}}(n)$ and $\hat{I}_{\text{out}}(n)$ are the real and imaginary parts of coefficients obtained from the trained DNN. The weights and biases of different neurons are updated by utilizing the Adam algorithm [17], until the MSE loss reaches a preset value or convergence.

III. Measurement Setup and Results

A. Measurement Setup

The block diagram and photograph of the measurement setup in the compact range chamber are shown in Fig. 2(a) and (b), respectively. A 100-MHz bandwidth 5G NR intermediate frequency (IF) signal centered at 3 GHz is generated by the R&S SMBV100B vector signal generator's arbitrary waveform generator function. Agilent E8247C generates a 12.5-GHz unmodulated signal, which is frequency-doubled to 25 GHz and used as a local oscillator (LO) signal. The active mixer KTX321840 is used to upconvert the IF signal to the 28-GHz carrier frequency, and the active

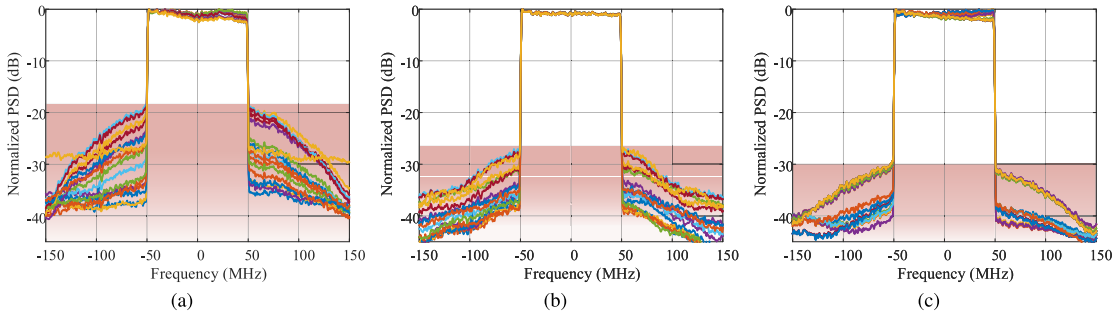

Fig. 3. Normalized PSDs. (a) AiP output without DPD. (b) AiP output with MPM DPD. (c) AiP output with MaD-DPD.

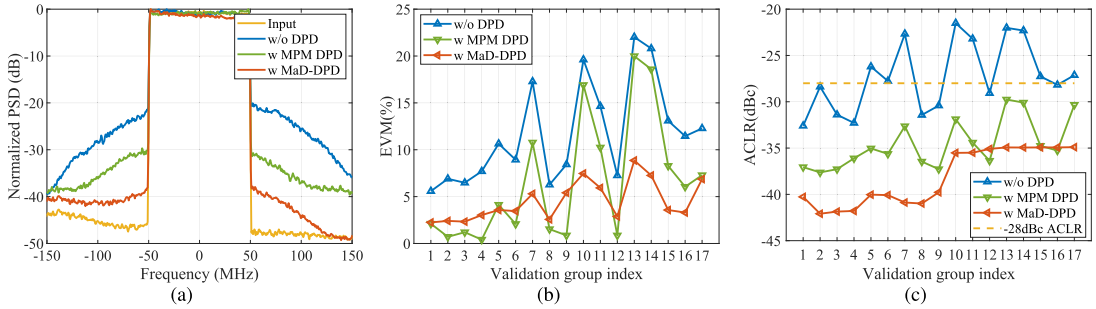

Fig. 4. Validation results of normalized PSD, EVM, and ACLR. (a) Normalized PSD of validation index 7 ($p = -21$ dBm, $\theta = 0°$). (b) EVM results of 17 validation group with (w) and without (w/o) DPD. (c) ACLR results of 17 validation group with (w) and without (w/o) DPD.

mixer KRX321840 is utilized to downconvert the signal back to IF. The high power is supplied by the pre-amplifier APH-26063325, which operates far below from its 1-dB compression point (more than 10 dB), and it is sufficient to drive the 4×4 AAiPK428GC-A0404 (AiP) close to saturation. The 28-GHz input signal oversampled by 600 MHz is fed to AiP, which includes four Anokiwave AWMF-0158 [18].

B. Validation Results and Analysis

There are 17 validations groups with varied input power and steering angle. After obtaining the MPM coefficients generated by the trained DNN and loading the calculated pre-distortion signals to the AiP, the normalized power spectral density (PSD) of the AiP output without DPD, with MPM DPD, and with MaD-DPD is shown in Fig. 3(a)–(c), respectively. From Fig. 3(b) and (c), it can be observed that after MPM DPD and MaD-DPD, the out-of-band distortion is significantly reduced. The performance of MaD-DPD is comparable with that of MPM DPD, or even being better. An exemplary case with the best performance can be obtained under the validation index of 7 ($p = -21$ dBm, $\theta = 0°$), which is shown in Fig. 4(a). As shown in Fig. 4(b), the EVM of MPM DPD and MaD-DPD can reach an average value of 4.94% and 4.50%, respectively. Fig. 4(c) illustrates the linearization performance in terms of adjacent channel leakage ratio (ACLR) measured through the total radiated power metric defined by 3GPP, where the ACLR limit of -28 dBc applies for systems operating at FR2 [19]. It can be seen that with the proposed MaD-DPD, the ACLR target is to be achieved within the entire considered input power and steering angle range. The MaD-DPD achieves the maximum linearization performance comparable to MPM DPD, which is due to that the DPD tends to increase the peak-to-average power ratio (PAPR) to compensate for nonlinearities within the APA. The envelope of the pre-distorted signal is clipped when it exceeds a specific threshold [20]. As shown in Fig. 5, the pre-distorted signal x_{DPD} generated by MaD-DPD has much lower PAPR than

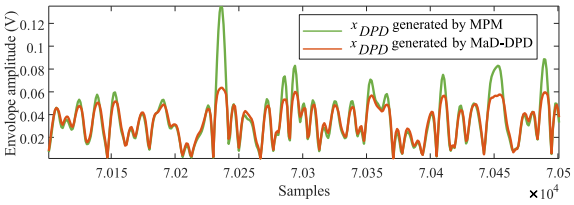

Fig. 5. Comparison of pre-distorted signal between MPM and MaD-DPD.

MPM. Therefore, the MaD-DPD avoids clipping and has a better performance than MPM DPD. Besides, the MaD-DPD avoids the need to acquire a large number of baseband I/Q signals, which is different from MPM DPD. When switching to other input power and steering angle, a large number of I/Q signals need to be reacquired to update the pre-distortion signal. Therefore, the proposed MaD-DPD can significantly reduce the computational complexity and improve the updating efficiency.

IV. Conclusion

In this letter, we propose an MaD-DPD method for the linearization of APA subjects to varied input power and steering angle. This method features the reliability and explainability contributed by conventional MPM DPD techniques and takes the full advantage of DNN to process the complex operation status of the APA with varied power levels and steering angles. The proposed method is implemented by only two variable state parameters and MPM coefficients. This eliminates the need for capturing and processing the I/Q data in application. Therefore, the proposed MaD-DPD can significantly reduce the computational complexity and improve the updating efficiency.

References

[1] A. Brihuega, L. Anttila, and M. Valkama, "Neural-network-based digital predistortion for active antenna arrays under load modulation," *IEEE Microw. Wireless Compon. Lett.*, vol. 30, no. 8, pp. 843–846, Aug. 2020.

[2] B. Khan, N. Tervo, A. Parssinen, and M. Juntti, "Average linearization of phased array transmitters under random amplitude and phase variations," in *Proc. 16th Int. Symp. Wireless Commun. Syst. (ISWCS)*, Aug. 2019, pp. 553–557.

[3] X. Hu, Z. Liu, W. Wang, M. Helaoui, and F. M. Ghannouchi, "Low-feedback sampling rate digital predistortion using deep neural network for wideband wireless transmitters," *IEEE Trans. Commun.*, vol. 68, no. 4, pp. 2621–2633, Apr. 2020.

[4] X. Yu, X. Hu, Z. Liu, C. Wang, W. Wang, and F. M. Ghannouchi, "A method to select optimal deep neural network model for power amplifiers," *IEEE Microw. Wireless Compon. Lett.*, vol. 31, no. 2, pp. 145–148, Feb. 2021.

[5] X. Liu *et al.*, "Beam-oriented digital predistortion for 5G massive MIMO hybrid beamforming transmitters," *IEEE Trans. Microw. Theory Techn.*, vol. 66, no. 7, pp. 3419–3432, Jul. 2018.

[6] C. Yu *et al.*, "Full-angle digital predistortion of 5G millimeter-wave massive MIMO transmitters," *IEEE Trans. Microw. Theory Techn.*, vol. 67, no. 7, pp. 2847–2860, Jul. 2019.

[7] C. Li, S. He, F. You, J. Peng, and P. Hao, "Analog predistorter averaged digital predistortion for power amplifiers in hybrid beamforming multi-input multi-output transmitter," *IEEE Access*, vol. 8, pp. 146145–146153, 2020.

[8] N. Tervo *et al.*, "Combined sidelobe reduction and omnidirectional linearization of phased array by using tapered power amplifier biasing and digital predistortion," *IEEE Trans. Microw. Theory Techn.*, vol. 69, no. 9, pp. 4284–4299, Sep. 2021.

[9] R. Hongyo, Y. Egashira, T. M. Hone, and K. Yamaguchi, "Deep neural network-based digital predistorter for Doherty power amplifiers," *IEEE Microw. Wireless Compon. Lett.*, vol. 29, no. 2, pp. 146–148, Feb. 2019.

[10] P. Miao, B. Zhu, C. Qi, Y. Jin, and C. Lin, "A model-driven deep learning method for LED nonlinearity mitigation in OFDM-based optical communications," *IEEE Access*, vol. 7, pp. 71436–71446, 2019.

[11] X. Hu, Z. Liu, W. Wang, M. Helaoui, and F. M. Ghannouchi, "Low-feedback sampling rate digital predistortion using deep neural network for wideband wireless transmitters," *IEEE Trans. Commun.*, vol. 68, no. 4, pp. 2621–2633, Apr. 2020.

[12] *3GPP, User Equipment (UE) Radio Transmission and Reception—Part 3: Range 1 and Range 2 Interworking Operation With Other Radios, 2019, TS 38.101-3 Version 16.0.0 Release 16*. Accessed: Jan. 5, 2021. [Online]. Available: https://ieeexplore.ieee.org/document/9314547

[13] Y. LeCun, Y. Bengio, and G. E. Hinton, "Deep learning," *Nature*, vol. 521, pp. 436–444, Dec. 2015.

[14] Y. Li *et al.*, "A cross-mode universal digital pre-distortion technology for low-sidelobe active antenna arrays in 5G and satellite communications," *Electronics*, vol. 10, no. 16, p. 2031, Aug. 2021.

[15] M. U. Hadi, P. A. Traverso, G. Tartarini, O. Venard, G. Baudoin, and J.-L. Polleux, "Digital predistortion for linearity improvement of VCSEL-SSMF-based radio-over-fiber links," *IEEE Microw. Wireless Compon. Lett.*, vol. 29, no. 2, pp. 155–157, Feb. 2019.

[16] D. Wang, M. Aziz, M. Helaoui, and F. M. Ghannouchi, "Augmented real-valued time-delay neural network for compensation of distortions and impairments in wireless transmitters," *IEEE Trans. Neural Netw. Learn. Syst.*, vol. 30, no. 1, pp. 242–254, Jun. 2019.

[17] D. P. Kingma and J. Ba, "Adam: A method for stochastic optimization," Dec. 2014, *arXiv:1412.6980*.

[18] Anokiwave. (2019). *AWMF-0158 28 GHz Silicon 5G Tx/Rx Quad Core IC*. [Online]. Available: https://www.anokiwave.com/products/awmf-0158/index.html

[19] *NR; Base Station (BS) Radio Transmission and Reception*, Standard 3GPP Tech. Spec. 38.104, v15.4.0 (Release 15), Dec. 2018.

[20] R. N. Braithwaite, "A combined approach to digital predistortion and crest factor reduction for the linearization of an RF power amplifier," *IEEE Trans. Microw. Theory Techn.*, vol. 61, no. 1, pp. 291–302, Jan. 2013.